

# Thermal Characterization of Epoxy Nanocomposites Containing Polyhedral Oligomeric Silsesquioxane: Glass Transition Temperature and Chemical Conversion

Puzhong Gu, Guang Yang<sup>1</sup>, Sang Cheol Lee<sup>2</sup>, and Jong Keun Lee<sup>2\*</sup>

College of Materials Science and Engineering, Nanjing Tech University, Nanjing 210009, China

<sup>1</sup>Institute for Sports Research, Nanyang Technological University, Singapore 639798, Singapore

<sup>2</sup>Department of Polymer Science and Engineering, Kumoh National Institute of Technology, Gumi 39177, Korea

(Received May 30, 2016; Accepted November 15, 2016)

**Abstract:** An epoxy resin (diglycidyl ether of bisphenol-A) was blended with different loadings of a glycidyl-polyhedral oligomeric silsesquioxane (POSS) and isothermally cured with an amine hardener at varying temperatures and times. The glass transition temperature ( $T_g$ ) of the samples was measured at different chemical conversions ( $\alpha$ ) using differential scanning calorimetry (DSC). Time-temperature shifts were made for  $T_g$  vs.  $\ln(\text{time})$  data to be superposed at an arbitrary reference temperature in the kinetically controlled reaction regime, and these shift factors were used to obtain an Arrhenius activation energy. The influence of POSS on different reaction systems was investigated in terms of the  $T_g$ - $\alpha$  relationship, which was fitted with two models; DiBenedetto and Venditti/Gillham equations. It was found that POSS molecules played different roles at different stages of the curing process. At lower conversions, the inorganic cage of the incorporated POSS (up to 20 wt%) reduced the mobility of the molecular segments, giving rise to an increase in  $T_g$ . However, above the 20 wt% POSS, there was a depression of  $T_g$ , which may be associated with a plasticizing effect of organic substituents of the POSS molecules. Moreover, the effect of POSS on  $T_g$  became less pronounced when the conversion reached 0.8.

**Keywords:** Epoxy, Polyhedral oligomeric silsesquioxane (POSS), Glass transition temperature, Chemical conversion, Differential scanning calorimetry (DSC)

## Introduction

For thermosetting materials, amorphous solids with a high molecular weight are generally formed from liquids with a low molecular weight *via* a variety of chemical reactions. The curing process is important in the fabrication of structural composites, coatings, adhesives, and electronic encapsulants [1,2]. As a cure reaction proceeds, the glass transition temperature ( $T_g$ ) gradually increases and reaches a maximum where a fully crosslinked structure emerges. In order to design optimum cure cycles and acquire desirable properties for thermosetting materials, understanding the curing process is of particular importance. It is well-known that the glass transition temperature is a useful metric in monitoring the cure process of an epoxy/amine system, due to the one-to-one relationship between  $T_g$  and chemical conversion ( $\alpha$ ) [3]. From an analysis of the variation of  $T_g$  and  $\alpha$  under isothermal cure conditions, a direct and deep insight into cure kinetics of thermosetting systems can be displayed through information on activation energy, state of cure, reaction mechanism, etc.

Organic-inorganic hybrid materials have recently attracted a great deal of attention from the standpoint of their potentially improved properties. These nanocomposites generally exhibit a better performance than the sum of their individual components [4,5]. An ideal candidate material for the preparation of hybrid materials is polyhedral oligomeric

silsesquioxane (POSS), which is inorganic silica-like nanocage molecules with organic substituents at eight vertices, one or more of which is capable of copolymerization. These resulting hybrid materials have the advantage of being covalently linked to polymer chains via curing or grafting reactions, leading to moderate control of POSS aggregation [6,7]. POSS with inactive substituents can also promote physical dispersion in the organic matrix at a molecular level [8].

Epoxy is a class of important engineering resins with widespread use due to its ease of fabrication, favorable mechanical properties, excellent chemical resistance, and low cost [9]. POSS has been applied in a large number of thermoplastic and thermosetting polymer matrices, among which epoxy/POSS hybrids are some of the more extensively investigated systems [10]. The incorporation of POSS into an epoxy resin provides the hybrid material with superior thermo-mechanical properties [10-13]. Lee and Lichtenhan [11] studied the thermal and viscoelastic properties of bisphenol-A type epoxy containing cyclohexyl (or cyclopentyl) POSS. Significant retardation of the physical aging process in the glassy state was observed for the samples reinforced by the POSS cages due to the reduction of segmental mobility in the epoxy networks. A liquid-liquid phase separation was observed in the preparation of epoxy composites containing glycidyl isobutyl POSS, indicating the incompatibility between the epoxy resin and POSS [12]. Monofunctional or multifunctional POSS-epoxides have been incorporated into epoxy resins, leading to improvements in the thermal and/or rheological properties of epoxy resins [8,13].

\*Corresponding author: jklee@kumoh.ac.kr

There have been studies on the glass transition temperature of epoxy/POSS nanocomposites displaying enhanced or reduced  $T_g$ . The  $T_g$  of the octakis (dimethylsiloxypropylglycidyl ether)silsesquioxane/1,3-phenylenediamine(mPDA) system was significantly higher than that of the neat matrix material due to the POSS cages hindering the motion of the chains [14]. The increased  $T_g$  of the POSS loaded samples is likely caused by the high cross-linking density that results from the bonding of the organic tethers of POSS to the polymer network [15]. On the contrary, Li *et al.* [13] reported that an epoxy matrix composite incorporated with a multifunctional POSS (at 25 wt%) showed a lower  $T_g$  than the neat epoxy, which is attributed to the reduced chemical conversion of the epoxy due to the POSS cages. Moreover, POSS nanocomposites exhibited decreased  $T_g$ , which is the result of plasticization effects caused by excess amounts of POSS [16]. The presence of POSS molecules could also lead to decreased  $T_g$  due to their hindering of the networks during polymerization [17].

To date, most of the work on the  $T_g$  of POSS-based epoxy composites has focused on fully cured samples. In this work, we report the effects of multifunctional POSS on an epoxy resin/amine hardener system in various stages of the curing process by measuring  $T_g$  and chemical conversion after isothermal curing using differential scanning calorimetry (DSC). The  $T_g$  and conversion data of the reaction systems are analyzed and discussed using time-temperature superposition, and fitted using Debenedetto and Venditti/Gillham models.

## Experimental

### Materials

The system being studied is based on a diglycidyl ether of bisphenol A type epoxy resin (DGEBA, YD-128, epoxy equivalent weight=184 g/eq, Kukdo Chemical, Korea) with an amine curing agent (mPDA, molecular weight=108 g/mol, Sigma-Aldrich, USA). A glycidyl-POSS filler (formula weight=1337.88 g/mol, Hybrid Plastics, USA) was added to the epoxy system. All components were used as received and are listed in Table 1.

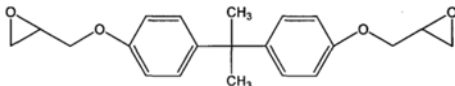
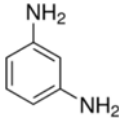
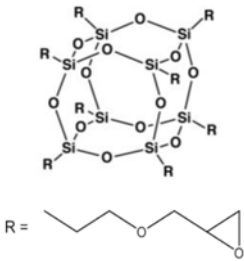
### Sample Preparation

For samples with different loadings of POSS, DGEBA and POSS were first heated to 70 °C and blended to obtain a homogeneous mixture with a magnetic stirrer. mPDA was then added into the DGEBA/POSS mixture and mechanically mixed for 10 min at 70 °C. These mixtures were immediately sealed in vials and placed in a freezer at -80 °C to prevent undesired curing prior to use. Note that the molar ratio of epoxide groups from DGEBA and glycidyl POSS to amine groups from mPDA for mixing is equal to one.

### DSC Measurements

DSC (200 F3, NETZSCH, Germany) was employed to

**Table 1.** Chemical structures of reactants used in this study

|          |   |
|----------|---|
| Epoxy    |  |
|          | DGEBA   |
| Hardener |  |
|          | mPDA  |
| Filler   |  |
|          | glycidyl-POSS   |

measure the glass transition temperature and the chemical conversion. A frozen mixture described above was warmed to room temperature, and approximately 10-15 mg of the mixture was put into a DSC pan and then sealed by crimping. The sealed pan was placed into the DSC cell and isothermally cured at curing temperatures ( $T_{cure}$ ) of 60, 80, 100, and 120 °C for curing times ( $t_{cure}$ ) of up to 360 min. Subsequently, a dynamic scan from -60 to 300 °C at a heating rate of 10 °C/min was performed to determine  $T_g$  and the residual reaction heat ( $\Delta H_r$ ). All experiments were done under a dry  $N_2$  atmosphere. The  $T_g$  and the heat of reaction were determined from the mid-point of the endothermic stepwise transition and the area under the exothermic peak on the DSC curves, respectively. From  $\Delta H_r$  for the isothermally cured sample and the total heat of reaction ( $\Delta H_T$ ) for unreacted samples, the fractional chemical conversion ( $\alpha$ ) was calculated using equation (1)

$$\alpha = 1 - \frac{\Delta H_r}{\Delta H_T} \quad (1)$$

When the chemical conversion of a thermoset material approaches 100 % (or complete curing), the  $T_g$  of the thermoset material reaches a maximum value  $T_{g\infty}$ . To obtain  $T_{g\infty}$  for samples containing 0, 10, 20, and 50 wt% of POSS, each sample was subjected to temperature cycles at a heating rate of 10 °C/min and a cooling rate of 40 °C/min. Samples were initially raised to 60 °C and then cooled quickly down to room temperature. Subsequent cycles were conducted by progressively raising the maximum temperature to higher temperatures (20 °C interval) up to 300 °C.  $T_g$  increased with

each progressive cycle until reaching a constant value, which can be taken as  $T_{g\infty}$ .

### Results and Discussion

#### Cure Behavior

Dynamic measurements were performed for epoxy/POSS samples with different POSS amounts (0, 10, 20, and 50 wt%)

uncured and isothermally cured at varying temperatures ( $T_{cure}=60-120\text{ }^{\circ}\text{C}$ ) for varying cure times ( $T_{cure}=0-360\text{ min}$ ). Typical DSC scans of the 20 wt% POSS loaded sample at  $T_{cure}=80\text{ }^{\circ}\text{C}$  for different curing times are shown in Figure 1. When samples vitrify at  $T_{cure}$  above  $T_g$  for prolonged curing times, sub- $T_g$  physical aging is known to occur [18]. Because of the physical aging, the endothermic peak appears in the glass transition region. In this work, the endothermic

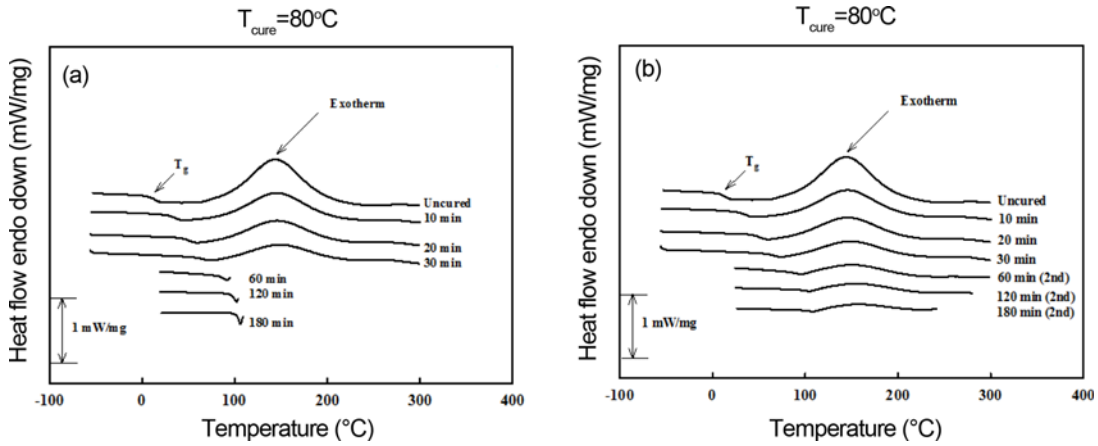


**Figure 1.** Dynamic DSC thermograms of 20 wt% POSS loaded samples isothermally cured at 80 °C for varying cure times; (a) the first scan only and (b) the first and the second scans.

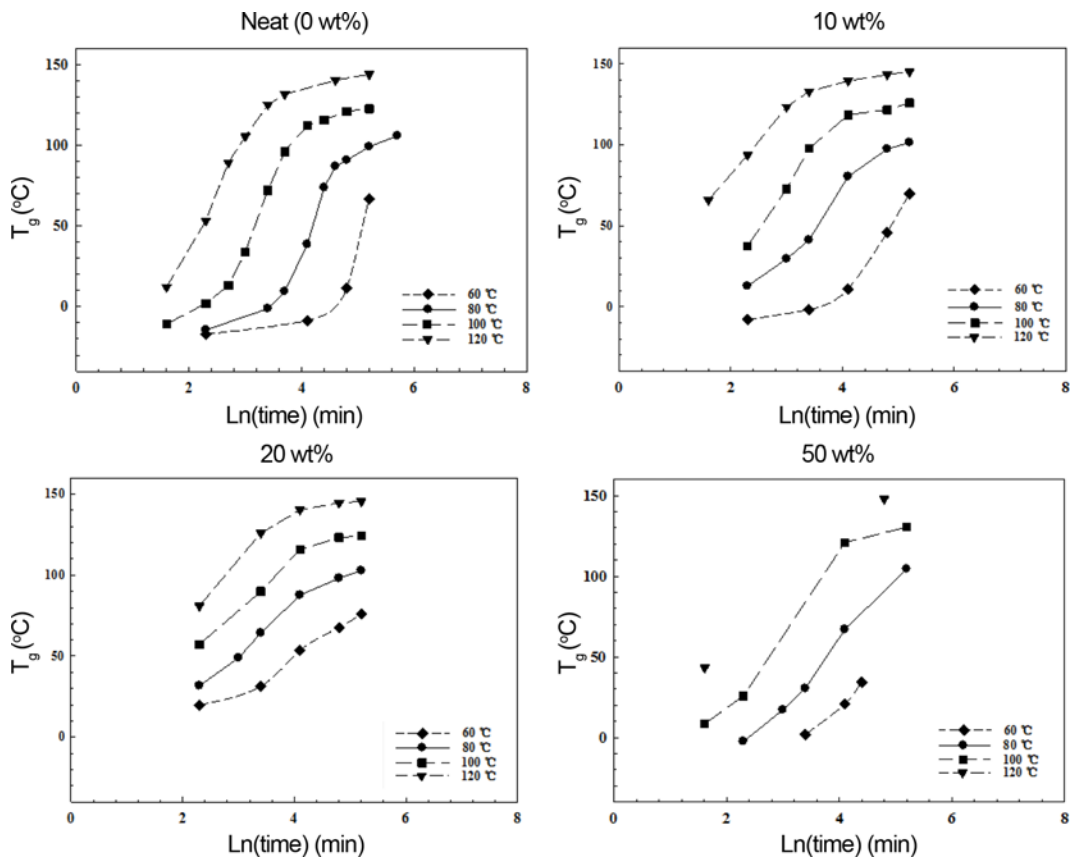


**Figure 2.**  $T_g$  vs.  $\ln(\text{time})$  for epoxy samples with 0, 10, 20, and 50 wt% POSS.

peak appears for the samples cured at a temperature of 80 °C for longer cure times ( $T_{\text{cure}}=60, 120, 180$  min; see Figure 1(a)). If so, these samples were quickly cooled from temperatures just above the endothermic peak to room temperature, and then immediately rescanned as shown in Figure 1(b). The endothermic aging peak, which complicates the assignment of  $T_g$ , was eliminated through the above procedures. Other samples containing different POSS loadings cured at different temperatures exhibit similar behavior. Moreover, for different sample formulations under different curing conditions, increasing  $T_g$  and decreasing exothermic peak areas were observed as the cure advanced with cure time.

### $T_g$ and Chemical Conversion vs. Ln(Time)

Owing to dramatic changes in the physical properties of thermosetting materials from the glassy state to the rubbery state during curing process,  $T_g$  is one of the important material parameters reflecting the thermo-mechanical properties. For thermosetting materials, the glass transition temperature gradually increases from the  $T_g$  value of the uncured monomer ( $T_{g0}$ ) to that of the fully reacted polymer ( $T_{g\infty}$ ) over the course of chemical conversions [17,18]. In Figure 2, the glass transition temperatures were plotted vs. ln(time) for

epoxy samples loaded with 0, 10, 20 and 50 wt% POSS. Prior to cure reaction,  $T_{g0}$  values were found to be -17, -2.4, 13.9 and -15 °C for epoxy samples with 0, 10, 20 and 50 wt% POSS, respectively. Notice a significant increase of 30.9 °C in  $T_{g0}$  for the 20 wt% POSS loaded sample relative to the neat epoxy sample, which is likely caused by the restriction of epoxy molecules by the inorganic POSS cages. As seen from this figure,  $T_g$  values progressively increase with the cure time and level off to limiting values for all samples tested, although some  $T_g$  values were not available for 50 wt% POSS loaded samples. In comparison with the neat epoxy sample, POSS loaded samples show higher  $T_g$  at the initial stage of curing, but approach nearly identical values at the later stages of curing when  $T_g$  reaches a limiting value. This indicates an acceleration effect of POSS on the curing reaction. Figure 3 represents the resulting conversion for epoxy samples with 0, 10, 20, and 50 wt% POSS, isothermally cured at different temperatures and for different times. Consistent with the  $T_g$  behavior, conversion also increased with increasing curing temperatures and times and leveled off thereafter. During the reaction of the epoxy resins, gelation and vitrification are known to occur. Once vitrification occurs ( $T_g=T_{\text{cure}}$ ), the reaction becomes diffusion controlled (as opposed to kinetically controlled) and any

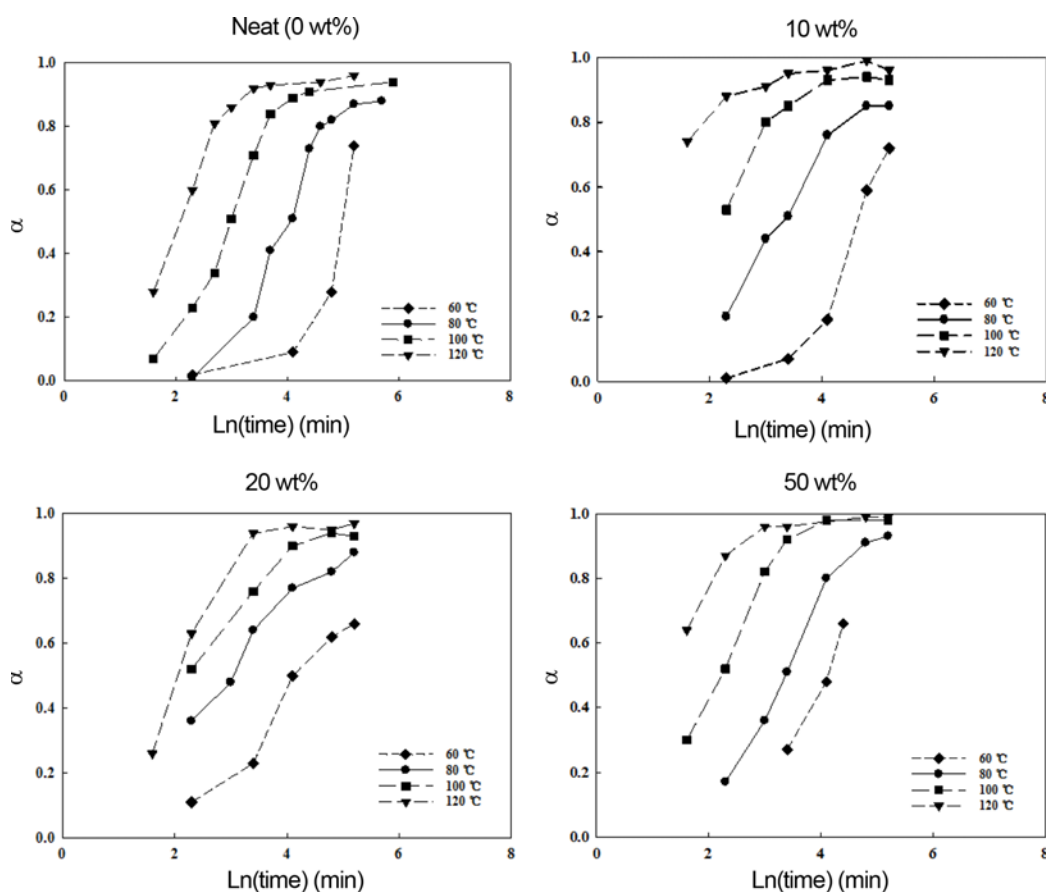


**Figure 3.**  $\alpha$  vs. ln(time) for epoxy samples with 0, 10, 20, and 50 wt% POSS.

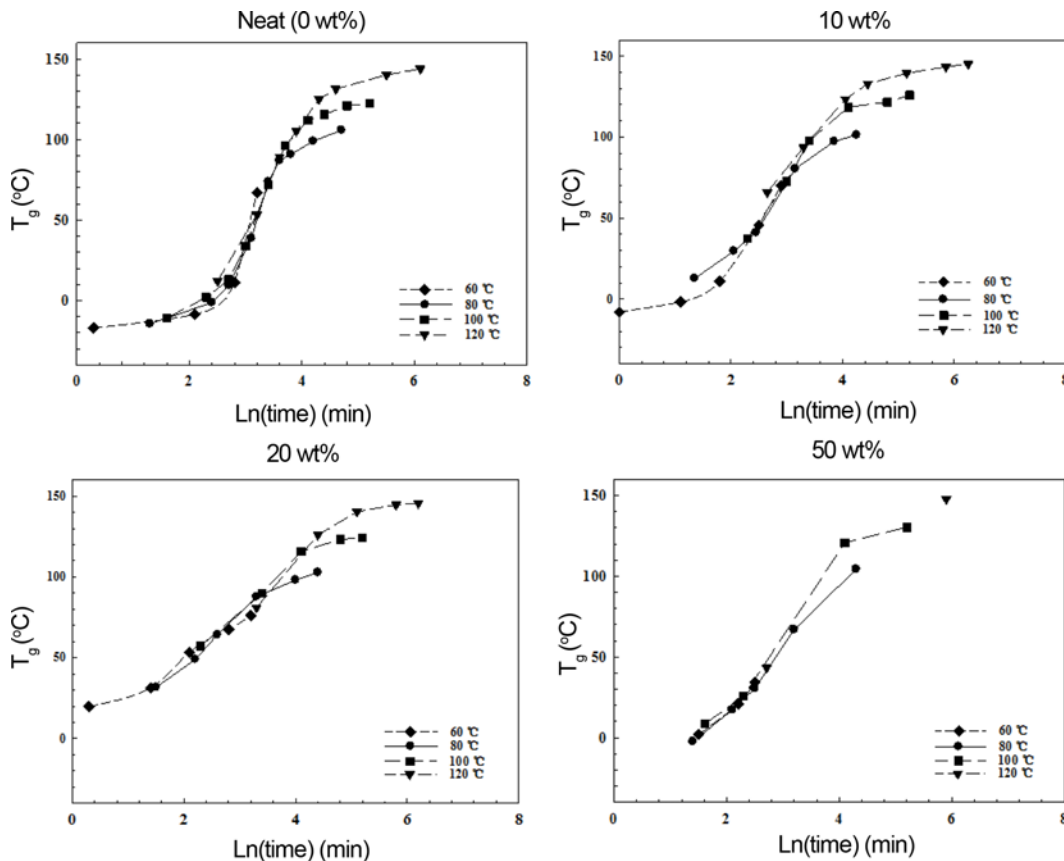


**Figure 4.** Superposition of the  $T_g$  vs.  $\ln(\text{time})$  data to form a master curve ( $T_{ref}=100^\circ\text{C}$ ) for epoxy samples with 0, 10, 20, and 50 wt% POSS.

substantial reactions stop, thus limiting further increases in  $T_g$  and conversion [19]. The level-off of the  $T_g$  and conversion with time in this work is closely related to the vitrification.

**Shifts of  $T_g$  and Activation Energy**

In order to coincide with the  $T_g$ - $\ln(\text{time})$  curve of  $T_{cure}=100^\circ\text{C}$  (as a reference temperature) in Figure 2, other curves were processed through horizontal shifts along  $\ln(\text{time})$  for the kinetically controlled beginning stage of each curve. The results of these horizontal shifts are shown in Figure 4. It can be noted that the shifted  $T_g$  data for all samples can be superimposed to produce a master curve prior to  $T_g=-85^\circ\text{C}$ , above which the  $T_g$  data branch off from the master curve due to the effect of the transition from kinetically control to diffusion control [3,20].

It has been previously reported that overall activation energy in thermosetting systems can be determined using the shifts of  $T_g$  vs. cure time at different isothermal temperatures, assuming that reaction is only kinetically controlled without any diffusion effects [18,21]. All  $T_g$  vs.  $\ln(\text{time})$  curves at different cure temperatures should be superimposable by horizontal shift at an arbitrary reference temperature ( $T_{ref}$ ) by a shift factor. The equation for the  $\ln(\text{time})$  shift factors,

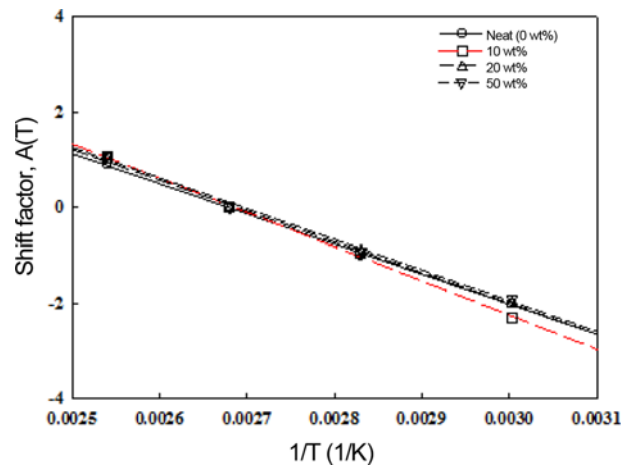


**Figure 5.** Shift factor vs.  $1/T$  for epoxy samples with 0, 10, 20, and 50 wt% POSS.

$A(T)$ , is related to the inverse of absolute temperature [21,22],

$$A(T) = \left(\frac{-E_a}{R}\right) \left(\frac{1}{T_{cure}} - \frac{1}{T_{ref}}\right) \tag{2}$$

where  $E_a$  is the apparent activation energy for the overall reaction, and  $R$  is the universal gas constant.

The  $\ln(\text{time})$  shift factors vs.  $1/T$  are shown in Figure 5. The activation energy for the reaction was determined from the slope of a fitting line based on the resulting points. The activation energies obtained in this work were 52.3, 59.5, 53.4 and 53.3 kJ/mol for epoxy samples with 0, 10, 20 and 50 wt% POSS, respectively. The activation energy of the DGEBA/mPDA system is in agreement with values reported in other studies using isothermal analysis [23]. It is interesting to note that the POSS loaded samples show higher activation energies relative to the neat epoxy system, with a maximum at a POSS loading of 10 wt%. This can be explained by the chemical structure of POSS molecules; the POSS molecule has a hybrid structure containing an inorganic Si-O cage center with organic side groups (R). The inorganic cage in POSS may decrease the mobility of reactive groups, increasing the activation energy. The low molecular weight of the flexible organic substituents may enhance the mobility of the functional groups, leading to a decrease in the activation energy. Therefore, the influence of the inorganic cages is dominant at a 10 wt% POSS loading, but the effect of the inorganic cage on activation energy is overridden by organic substituents at higher POSS loadings of 20 and 50 wt%.

### $T_g$ vs. Chemical Conversion

There are several investigations using the parameters  $T_g$  and  $\alpha$  to evaluate the isothermal cure behavior of epoxy resins [3,18,24]. According to previous reports, these two parameters are known to be in a unique one-to-one relationship. Figure 6 shows experimentally determined  $T_g$  data as a function of conversion, obtained from isothermally cured samples at different curing temperatures. This figure also contains  $T_g$  values for fully cured ( $T_{g\infty}$ ) samples determined by the successive temperature cycles. The  $T_{g\infty}$  values were found to be 169.0, 170.4, 174.9, and 169.2 °C for 0, 10, 20, and 50 wt% POSS loaded samples, respectively. There was a ~5 °C increase in  $T_g$  for the 20 wt% POSS loaded sample compared to the neat epoxy.

In this work,  $T_g$  vs.  $\alpha$  displays a similar trend to data found from other thermosetting materials [3,25]. The incorporation of POSS has a significant effect on  $T_g$  of reaction systems, especially at the beginning stages of the curing process.  $T_g$  values for 20 wt% POSS loaded samples exhibit maxima in the conversion range of  $\alpha \leq 0.8$  compared to those for neat epoxy and other POSS loaded samples. Note that the enhancement in  $T_g$  at a particular conversion becomes weaker as  $\alpha$  increases, i.e. the largest difference in  $T_g$  between the neat epoxy and POSS loaded samples was ~31 °C at  $\alpha=0$ , whereas the difference in  $T_g$  becomes ~5 °C at  $\alpha=1$ . The increased  $T_g$  could be explained by the nanoreinforcement of POSS cages within the polymer networks. When POSS cages have noncovalent attraction or chemical bonding within the polymer matrices, the segmental mobility of polymer chains around the nanofiller can be restricted, thus resulting in an improvement of  $T_g$  [26-28]. It is interesting to

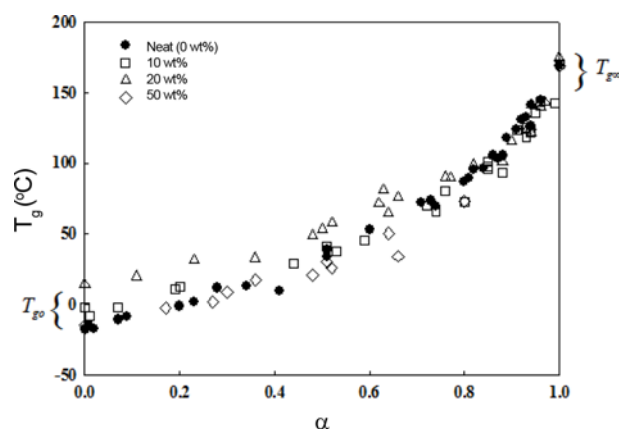


**Figure 6.**  $T_g$  vs.  $\alpha$  for epoxy samples with different POSS loadings at cure temperatures of 60, 80, 100, and 120 °C.

note that the reinforcement of POSS cages is more effective at lower conversions and becomes weaker as the conversion value increases.

### Effects of Curing Temperature and POSS Loading on $T_g$

The  $T_g$  vs.  $\alpha$  data in Figure 6 were replotted for the 20 wt% POSS loaded sample at different curing temperatures and for different POSS load amounts at  $T_{\text{cure}}=60$  °C, as shown in Figure 7. It is well known that there is a unique relationship between  $T_g$  and conversion, independent of cure temperature and thermal history [3,18]. Figure 7(a) shows all experimental  $T_g$  data as a function of conversion obtained from isothermally cured samples at different cure temperatures for the 20 wt% POSS loaded sample. From this figure, it is evident that  $T_g$  maintains a unique function of conversion independent of the cure temperature. As is well known, the reaction between epoxy and amine groups has multiple potential reaction mechanisms [29]. Therefore, the independence of  $T_g$  relative to the cure temperatures is likely caused either by the fact that multiple reactions occur simultaneously with comparable activation energies, or by the fact that these reactions take place in sequence (i.e., only one reaction proceeds at each stage of the curing process) [25,30]. As shown in Figure 7(b), the different  $T_g$  values were also monitored for different POSS loaded samples, indicating that  $T_g$  does not follow a unique function dependent on conversion. This implies that other effects influence  $T_g$  for epoxy/POSS systems. These factors are considered to be caused by the combination of the hindering effect of POSS cages (which increases  $T_g$ ) and the plasticizing effect of organic substituent in POSS (which decreases  $T_g$ ). Moreover, it was found that the maximum difference in  $T_g$  for different POSS loaded samples occurs at the lowest cure temperature studied (i.e.,  $T_{\text{cure}}=60$  °C). As  $T_{\text{cure}}$  increased, the  $T_g$  difference becomes smaller at higher cure temperatures and higher conversions. This indicates that a higher  $T_{\text{cure}}$  or higher conversion can diminish the positive effect of the POSS cages on  $T_g$ .

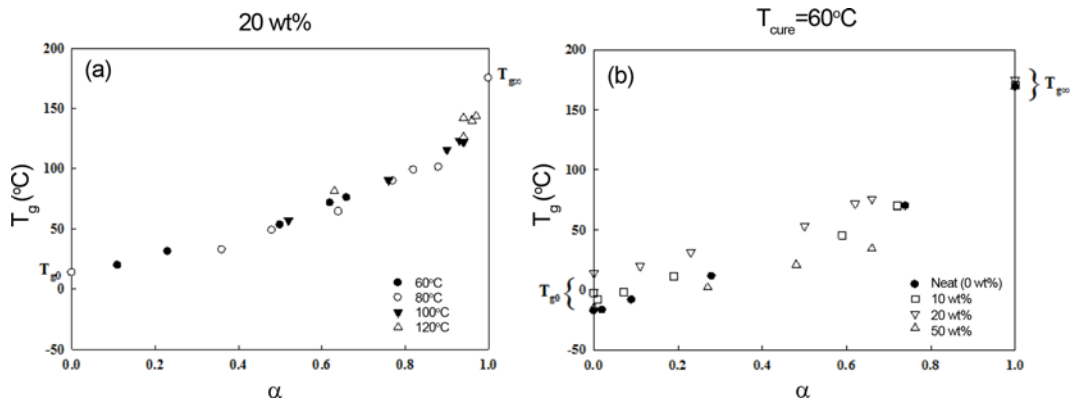


**Figure 7.**  $T_g$  vs.  $\alpha$  (a) for 20 wt% POSS loaded sample at different cure temperatures and (b) for different POSS loaded samples at  $T_{cure}=60^\circ\text{C}$ . Note that the  $T_{g\infty}$  values were determined from the temperature cycles.

**Relationship between  $T_g$  and Chemical Conversion**

For many thermosetting systems, a one-to-one relationship exists between  $T_g$  and chemical conversion independent of the curing temperature, and this relationship is generally nonlinear [21,24]. A temperature-independent  $T_g$ - $\alpha$  relationship implies that molecular structure remains unchanged or does not substantially affect  $T_g$  when cured at different temperatures. In order to provide a better understanding of the curing process over an entire conversion range, a mathematical  $T_g$  and  $\alpha$  relationship is given by the empirical DiBenedetto equation introduced by Nielsen and shown in equation (3) [25],

$$\frac{T_g - T_{g0}}{T_{g\infty} - T_{g0}} = \frac{\lambda\alpha}{1 - (1-\lambda)\alpha} \tag{3}$$

where  $T_{g0}$  and  $T_g$  are the glass transition temperatures of the unreacted ( $\alpha=0$ ) and the fully cured materials ( $\alpha=1$ ), respectively, and  $\lambda$  is an adjustable material constant.  $\lambda$  is defined as  $\Delta c_{p\infty}/\Delta c_{p0}$ , where  $\Delta c_{p0}=c_{p0}^l - c_{p0}^g$  and  $\Delta c_{p\infty}=c_{p\infty}^l - c_{p\infty}^g$  for  $\alpha=0$  and  $\alpha=1$ . The superscripts l and g refer to the liquid/rubbery state and glassy state, respectively.  $c_{p0}$  and  $c_{p\infty}$  are the specific heat capacities at constant pressure at  $\alpha=0$  and  $\alpha=1$ , respectively.

On the basis of thermodynamic considerations, Venditti

and Gillham [28] proposed an equation to predict the  $T_g$  vs. mole fraction of components for a linear copolymer [27,29]. The  $T_g$  and  $\alpha$  relationship is expressed for thermosetting materials as shown in equation (4) [3,31,32],

$$\ln(T_g) = \frac{(1-\alpha)\ln(T_{g0}) + \lambda\alpha\ln(T_{g\infty})}{(1-\alpha) + \lambda\alpha} \tag{4}$$

The difference in degrees of freedom for the motion of molecular chains between the liquid or the rubbery state and the glassy state can be reflected from  $\Delta c_p = c_p^l - c_p^g$  in  $\lambda$ . The stiffness of molecules can thus be qualitatively estimated from the magnitude of  $\Delta c_p$ . For flexible molecules, the  $\Delta c_p$  value is larger because the number of degrees of freedom in the liquid state is relatively larger than in the glassy state. On the contrary, fewer degrees of freedom in the liquid state results in a smaller  $\Delta c_p$  value in stiffer molecular systems. For thermosetting materials,  $\Delta c_p$  is large at a low molecular weight (relatively flexible). As the curing reaction proceeds, the molecules become stiffer as the molecular weight increases and crosslinks are formed, thus leading to a gradual decrease in  $\Delta c_p$  with conversion. By evaluating the  $\lambda$  values in different reaction systems, the stiffness of uncured and fully cured molecules can be compared. Figure 8 features the best fitted curves using the DiBenedetto and the Venditti/Gillham

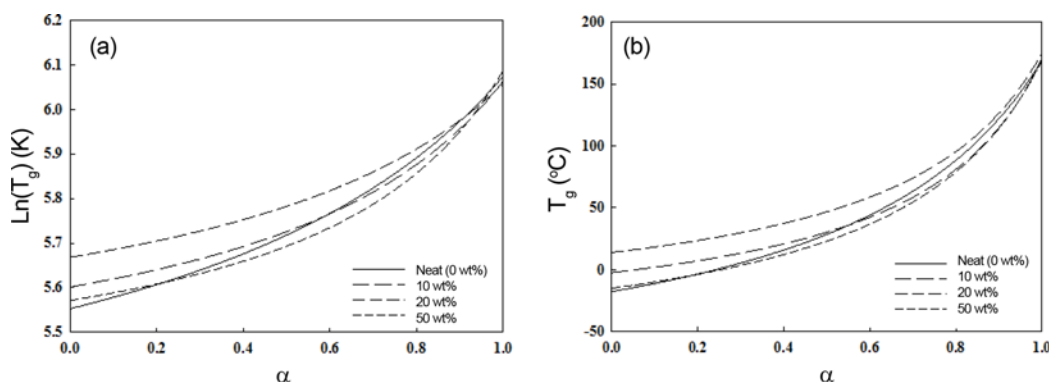


**Figure 8.** Fitted curves from the (a) DiBenedetto equation and (b) Venditti and Gillham equation for all samples.

**Table 2.** Predicted  $\lambda$  values using the DiBenedetto and Venditti/Gillham equations

| Sample       | DiBenedetto equation | Venditti/Gillham equation |
|--------------|----------------------|---------------------------|
| Neat (0 wt%) | 0.33±0.01            | 0.47±0.03                 |
| 10 wt%       | 0.23±0.01            | 0.37±0.03                 |
| 20 wt%       | 0.25±0.03            | 0.42±0.06                 |
| 50 wt%       | 0.26±0.02            | 0.31±0.04                 |

equations for 0, 10, 20 and 50 wt% POSS loaded samples at all investigated curing temperatures and for different times. Table 2 presents  $\lambda$  values obtained from the best fits of experimental  $T_g$  vs  $\alpha$  data using equations (3) and (4). For both fitted equations,  $\lambda$  values show similar trends as the POSS content is increased; a relatively significant decrease in  $\lambda$  at 10 wt% POSS relative to neat epoxy, and then a slight increase above 20 wt% POSS content. This means that the incorporation of POSS molecules leads to the stiffening of molecules, which is consistent with the observations of the increase in  $T_g$ .

The fitting curves from the DiBenedetto and Venditti/Gillham equations obtained previously were plotted together for all samples and shown in Figures 8(a) and (b), respectively. These two figures are quite similar in terms of the  $T_g$  vs.  $\alpha$  relationship. The POSS molecules have different influences on  $T_g$  at different stages of the curing process. At the beginning stage (below  $\alpha \sim 0.2$  for both equations), the  $T_g$  values of the nanocomposites are ordered as  $T_g$  (20 wt%) >  $T_g$  (10 wt%) >  $T_g$  (50 wt%) >  $T_g$  (neat). In the conversion range of  $\alpha = 0.2-0.55$  for the DiBenedetto equation and  $\alpha = 0.2-0.6$  for Venditti/Gillham equation, this order is  $T_g$  (20 wt%) >  $T_g$  (10 wt%) >  $T_g$  (neat) >  $T_g$  (50 wt%). When the conversion further increased to the end of the curing process, this is  $T_g$  (20 wt%) >  $T_g$  (neat) >  $T_g$  (10 wt%) >  $T_g$  (50 wt%). The changes in  $T_g$  with conversion can be interpreted by the combined effects of POSS on  $T_g$ .  $T_g$  increases due to the hindrance of molecular motion by the POSS inorganic cages, and  $T_g$  decreases due to the plasticizing effect of the POSS organic substituents.

### Conclusion

Epoxy nanocomposites containing octa(propylglycidyl ether) POSS up to 50 wt% were isothermally cured at different curing temperatures and for different times. The  $T_g$  and corresponding chemical conversion of samples uncured and partially cured were determined using DSC. The horizontal shift of  $T_g$  vs.  $\ln(\text{time})$  data at a reference temperature formed a master curve at the initial stage of curing (i.e., kinetically-controlled regime) and branched off at later stages of curing (i.e., diffusion-controlled regime) for all samples tested. Activation energies obtained in this work were 52.3, 59.5, 53.4 and 53.3 kJ/mol for 0, 10, 20 and

50 wt% POSS loaded samples, respectively. The experimental  $T_g$  values were also plotted as a function of  $\alpha$  and curve-fitted with the well-known DiBenedetto and Venditti/Gillham equations, for determining the  $T_g$ - $\alpha$  relationship and analyzing the effect of POSS in the whole conversion range. It was found that POSS molecules have different effects on  $T_g$  at different stages of cure. At the beginning stage of curing ( $\alpha < 0.2$ ), the nanocomposites exhibited  $T_g$  values in the order of  $T_g$  (20 wt%) >  $T_g$  (10 wt%) >  $T_g$  (50 wt%) >  $T_g$  (neat). At the conversion range of  $\alpha = 0.2-0.55$  for the DiBenedetto equation and  $\alpha = 0.2-0.6$  for Venditti/Gillham equation, this order was  $T_g$  (20 wt%) >  $T_g$  (10 wt%) >  $T_g$  (neat) >  $T_g$  (50 wt%). Above this range, this order was  $T_g$  (20 wt%) >  $T_g$  (neat) >  $T_g$  (10 wt%) >  $T_g$  (50 wt%). The effect of POSS on  $T_g$  can be explained by the combined effects of hybrid characteristics of the POSS inorganic and organic segments. The inorganic Si-O cage was responsible for the enhanced  $T_g$  due to the restriction of segmental mobility at lower conversion values (or lower molecular weights) and the organic substituent was for the reduced  $T_g$  due to the incorporation of the flexible segment into the matrix chains at higher conversion values.

### Acknowledgements

This work was supported by a research fund from Kumoh National Institute of Technology.

### References

1. K. L. Forsdyke and T. F. Starr, "Thermoset Resins", iSmithers Rapra Publishing, 2002.
2. J. Zeng, "DSC Studies of Cure Kinetics for Epoxy-amine Systems and Measurements of Toughness for Epoxy-based Materials", Kansas State University, 1995.
3. G. Wisanrakkit and J. Gillham, *J. Appl. Polym. Sci.*, **41**, 2885 (1990).
4. C. Sanchez and P. Gómez-Romero in "Functional Hybrid Materials" (C. Sanchez and P. Gómez-Romero Eds.), p.1, Wiley-VCH, Germany, 2004.
5. J. Choi, S. G. Kim, and R. M. Laine, *Macromolecules*, **37**, 99 (2004).
6. A. Waddon, L. Zheng, R. Farris, and E. B. Coughlin, *Nano Lett.*, **2**, 1149 (2002).
7. L. Zheng, A. J. Waddon, R. J. Farris, and E. B. Coughlin, *Macromolecules*, **35**, 2375 (2002).
8. J. D. Lichtenhan, J. J. Schwab, and W. A. Reinert, *Chem. Innov.*, **31**, 3 (2001).
9. K. Y. Mya, C. He, J. Huang, Y. Xiao, J. Dai, and Y. P. Siow, *J. Polym. Sci. Pol. Chem.*, **42**, 3490 (2004).
10. Y. Liu, S. Zheng, and K. Nie, *Polymer*, **46**, 12016 (2005).
11. A. Lee and J. D. Lichtenhan, *Macromolecules*, **31**, 4970 (1998).
12. M. J. Abad, L. Barral, D. P. Fasce, and R. J. Williams,



- Macromolecules*, **36**, 3128 (2003).
13. G. Z. Li, L. Wang, H. Toghiani, T. L. Daulton, K. Koyama, and C. U. Pittman, *Macromolecules*, **34**, 8686 (2001).
  14. W. Y. Chen, Y. Z. Wang, S. W. Kuo, C. F. Huang, P. H. Tung, and F. C. Chang, *Polymer*, **45**, 6897 (2004).
  15. J. K. H. Teo, K. C. Teo, B. Pan, Y. Xiao, and X. Lu, *Polymer*, **48**, 5671 (2007).
  16. H. Dodiuk, I. Blinsky, A. Dotan, and A. Buchman, *Int. J. Adhes. Adhes.*, **25**, 211 (2005).
  17. M. Urbaniak, *Polimery*, **56**, 240 (2011).
  18. G. C. Huang and J. K. Lee, *Compos. Pt. A-Appl. Sci. Manuf.*, **41**, 473 (2010).
  19. F. Boey and B. Yap, *Polym. Test.*, **20**, 837 (2001).
  20. J. Choi, J. Harcup, A. F. Yee, Q. Zhu, and R. M. Laine, *J. Am. Chem. Soc.*, **123**, 11420 (2001).
  21. P. I. Karkanias and I. K. Partridge, *J. Appl. Polym. Sci.*, **77**, 2178 (2000).
  22. E. Denardin, P. Janissek, and D. Samios, *Thermochim. Acta*, **395**, 159 (2002).
  23. V. Zvetkov, *Polymer*, **43**, 1069 (2002).
  24. F. Boey and W. Qiang, *J. Appl. Polym. Sci.*, **78**, 511 (2000).
  25. L. E. Nielsen, *J. Macromol. Sci. C Polym. Rev.*, **3**, 69 (1969).
  26. E. Giannelis, R. Krishnamoorti, and E. Manias, "Polymers in Confined Environments", p.107, Springer, 1999.
  27. T. S. Haddad and J. D. Lichtenhan, *Macromolecules*, **29**, 7302 (1996).
  28. F. Feher, K. Wyndham, R. Baldwin, J. Ziller, and J. Lichtenhan, *Chem. Commun.*, 1289 (1999).
  29. P. H. Lin and R. Khare, *Macromolecules*, **42**, 4319 (2009).
  30. X. Liu, X. Sheng, J. Lee, and M. Kessler, *J. Therm. Anal. Calorim.*, **89**, 453 (2007).
  31. S. Simon and J. Gillham, *J. Appl. Polym. Sci.*, **46**, 1245 (1992).
  32. A. Hale, C. W. Macosko, and H. E. Bair, *Macromolecules*, **24**, 2610 (1991).